No. 131/24, 23–35
ISSN 2657-6988 (online)
ISSN 2657-5841 (printed)
DOI: 10.26408/131.02

Submitted: 09.05.2023
Accepted: 20.12.2023
Published: 30.09.2024

SPEED VARIATION OF A CAGE INDUCTION MOTOR UNDER SQUARE VOLTAGE MODULATION

Piotr Gnaciński[1], Damian Hallmann[2*]

[1,2] Gdynia Maritime University, Morska 81–87, 81–225 Gdynia, Poland, Faculty of Electrical Engineering, Department of Marine Electrical Power Engineering

[1] ORCID 0000-0003-3903-0453, email: p.gnacinski@we.umg.edu.pl

[2] ORCID 0000-0003-4129-8336, email: d.hallmann@we.umg.edu.pl

*Corresponding author

Abstract: Cyclic voltage fluctuations can be considered as a superposition of the fundamental voltage component, subharmonic and interharmonic components – that is the components of frequency less than the fundamental one or not being its integer multiple. A commonly occurring case of voltage fluctuations is square voltage modulation. This paper deals with the effect of square voltage modulation on the rotational speed of an induction motor. The results of the FEM computations are presented for a cage induction motor with a rated power 3 kW and various parameters describing the voltage modulation.

Keywords: cage induction motor, finite element method, interharmonics, power quality, rotational speed, subharmonics, voltage fluctuations.

1. INTRODUCTION

Voltage fluctuations are considered to be one of the most significant and common power quality disturbances [Bollen and Gu 2006; Ghaseminezhad et al. 2021a,b; Kuwałek 2021b; Patel and Chowdhury 2021]. They are defined as rapid changes in the rms values of a voltage. Cyclic voltage fluctuations can be treated as the superposition of the fundamental component along with the additional components – subharmonics and interharmonics, i.e. components with a frequency lower than the fundamental component and the component with a frequency that is not an integer multiple of the fundamental frequency [Gallo et al. 2005; Bollen and Gu 2006; Tennakoon, Perera and Robinson 2008; IEEE Standard 1453-2015; Ghaseminezhad et al. 2021a,b].

In practice, it is equivalent to the occurrence of additional components in the voltage waveform [Gallo et al. 2005; Bollen and Gu 2006; Tennakoon, Perera and Robinson 2008; Ghaseminezhad et al. 2021a,b]. Depending on the phase angles of the subharmonic and interharmonic components, various cases of voltage modulation can be distinguished, like amplitude modulation, phase modulation and intermediate modulation [Gallo et al. 2005; Bollen and Gu 2006].

The most common voltage fluctuations are probably rectangular, in voltage flickers [Kuwałek 2021a; 2022]. Of note, when the voltage modulating function does not have a sinusoidal waveform, it can be considered a superposition of the sinusoids with different frequencies, amplitudes and phase shifts [Ghaseminezhad et al. 2021a,b].

The occurrence of voltage fluctuations is associated with the operation of time-varying power consumers and renewable energy sources [Bollen and Gu 2006; Kovaltchouk et al. 2016]. Subharmonics and interharmonics disturb various elements of the power system – power electronic equipment, light sources, power and measurement transformers, automation systems, synchronous and asynchronous machines [Gallo et al. 2005; Testa et al. 2007; Tennakoon, Perera and Robinson 2008; Ghaseminezhad et al. 2017a,b; 2021a,b; Gnaciński et al. 2019a,c; 2021; Gnaciński and Klimczak 2020; Hallmann 2020; Crotti et al. 2021; Gnaciński, Muc and Pepliński 2021; Zhang, Kang and Yuan 2021].

In asynchronous motors they cause an increase in power losses and winding temperature, local saturation of the magnetic circuit, vibrations, speed and torque fluctuations [Tennakoon, Perera and Robinson 2008; Ghaseminezhad et al. 2017a,b; 2021a,b; Gnaciński et al. 2019a,b,c; 2021; Gnaciński and Klimczak 2020; Hallmann 2020; Gnaciński, Muc and Pepliński 2021; Zhang, Kang and Yuan 2021]. Of note, speed fluctuations results in the flow of additional current subharmonics and interharmonics [Tennakoon, Perera and Robinson 2008; Ghaseminezhad et al. 2017a,b; Gnaciński et al. 2019a,b,c; 2021; Hallmann 2020].

For example, both current subharmonics and interharmonics flow through windings of a motor supplied with a voltage containing interharmonics. In some cases the extra current components additionally boost the speed fluctuations, leading to resonance phenomena [Gnaciński et al. 2019a,b,c; 2021; Hallmann 2020; Ghaseminezhad et al. 2021a,b]. It is also worth mentioning that the speed fluctuations (for example, caused by DC-link voltage fluctuations) may result in faulty operation of a frequency-controlled induction motor drive system [Zhang, Kang and Yuan 2021].

Voltage quality standards generally do not specify the permissible levels of subharmonics and interharmonics. [IEEE Standard 519 2020] provides only proposals for potential limit curves. In turn, the following comment is made in EN 50160 [EN 50160 2010]: ‘levels are under consideration, pending more experience’. In summary, the determination of permissible levels of subharmonics and interharmonics requires comprehensive studies on their impact on various elements of the power system.

Previous works on asynchronous motors supplied with the voltage containing subharmonics and interharmonics mainly concerned the single voltage subharmonic or interharmonic [Tennakoon, Perera and Robinson 2008; Gnaciński et al.

2019a,b,c; 2021; Gnaciński and Klimczak 2020] or the sinusoidal modulation of voltage amplitude [Tennakoon, Perera and Robinson 2008; Ghaseminezhad et al. 2017a,b; 2021a,b]. This paper presents the impact of rectangular voltage modulation on the speed fluctuations of a low-power induction motor. The scope of research was limited to amplitude modulation.

2. METHODOLOGY

For this paper a two-dimensional finite element method was applied. The model parameters of the investigated motor, TSg100L-4B, were identified on the grounds of design data and experimental results [Hallmann 2020], and then implemented in an ANSYS Electronics Desktop environment.

The motor ratings are provided in Table 1. The used tau-type mesh (Fig. 1) contained approximately 22,000 triangular elements, and its density was chosen based on the convergence analysis of the solution [Hallmann 2020]. Numerical computations were performed with a transient type solver.

A detailed description of the motor model is presented in Hallmann [2020] and Gnaciński et al. [2019b; 2021], with its experimental verification for the supply voltage containing subharmonics and interhamonics in Gnaciński et al. [2019a,b; 2021] and Hallmann [2020].

Table 1. Nominal data of tested motor type: TSg100L-4B

Parameter	Value
Rated power	3 kW
Rated frequency	50 Hz
Rated voltage	380 V
Rated current	6.9 A
Rated power factor	0.81
Rated speed	1420 rpm
Winding connection	delta

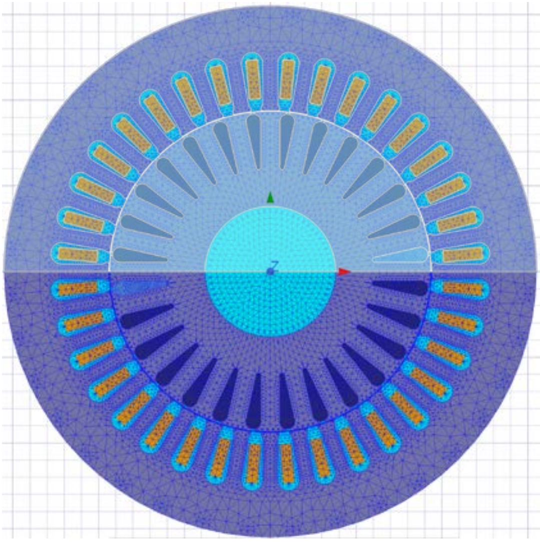

Fig. 1. Applied mesh

Source: own study.

3. SQUARE VOLTAGE MODULATION AND ROTATIONAL SPEED CHANGES

As mentioned in the Introduction, square voltage modulation can be treated as a superposition of various sinusoidal modulations [Ghaseminezhad et al. 2021a,b]). Each harmonic component of the modulating function causes subharmonic/interharmonic of frequency $f_{sh/ih}$ (based on [Gallo et al. 2005; Zhang, Xu and Liu 2005; Bollen and Gu 2006; Ghaseminezhad et al. 2021a,b]):

$$f_{sh/ih} = f_1 \mp k f_{mod} \tag{1}$$

where:

k – an integer,
f_1 – the fundamental frequency,
f_{mod} – the modulation frequency.

For f_{sh} described with the above expression greater than zero, the subharmonic/interharmonic component has a positive-sequence, otherwise a negative-sequence [Zhang, Xu and Liu 2005].

The instantaneous voltage value under amplitude modulation can be expressed as (based on [Bollen and Gu 2006]):

$$v(t) = x_{mod}(t) \cdot V_1 sin(2\pi f_1 t + \psi) \tag{2}$$

where:

V_1 – the amplitude of the fundamental component;
$x_{mod}(t)$ – the supply voltage modulation signal;
ψ – the initial phase angle of fundamental component.

For the purpose of this study, the modulating function $x_{mod}(t)$ is assumed as follows:

$$x_{mod}(t) = \begin{cases} 1.01; t \geq \frac{k}{f_m} \wedge t < \frac{k+DutyCycle}{f_m} \\ 0.99; t \geq \frac{k+DutyCycle}{f_m} \wedge t < \frac{k+1}{f_m} \end{cases} \tag{3}$$

where:

k – an integer value 0, 1, …, n;
T_m – the modulation period;
DutyCycle – the fill factor, described with the following dependency:

$$DutyCycle = \frac{t_1}{T_m} = t_1 f_m \tag{4}$$

The meaning of the time period t_1 is explained in Figure 2.

The results of investigations on speed fluctuations are presented below. All numerical experiments were performed for the load torque and the fundamental voltage component of rated values (T_n = 20.25 Nm and U_n = 380 V), and a moment of load inertia 15 times greater than the motor moment (motor moment of inertia J_s = 0.00702299 kg m^2; moment of load inertia J_o = 0.1317374 kg m^2).

Of note, this value was chosen since it corresponds to the moment of inertia of a DC generator coupled with the motor under research.

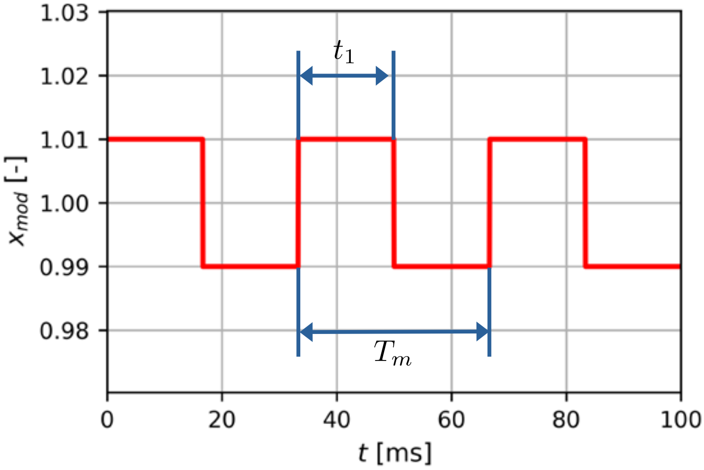

Fig. 2. Example of the modulating signal waveform for *DutyCycle* = 0.5
and voltage modulation frequency, f_m = 30 Hz

Example waveforms of the test voltage and its spectrum are presented in Figures 3 and 4, for the modulation frequency f_m = 30 Hz and the fill factor *DutyCycle* = 0.5. The subharmonic interharmonic of frequency 20 Hz and 80 Hz, present in the spectrum (Fig. 4) resulted from the first harmonic of the modulating function, while components of frequency 40 Hz and 130 Hz from the third harmonic.

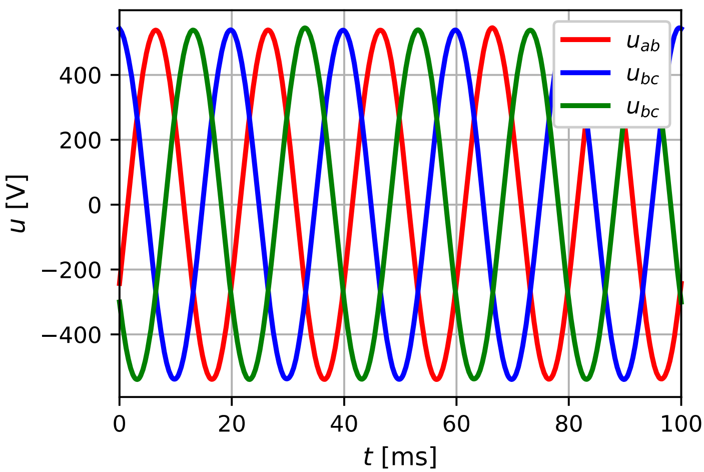

Fig. 3. Example of the test voltage waveform for *DutyCyle* = 0.5
and the voltage modulation frequency, f_m = 30 Hz

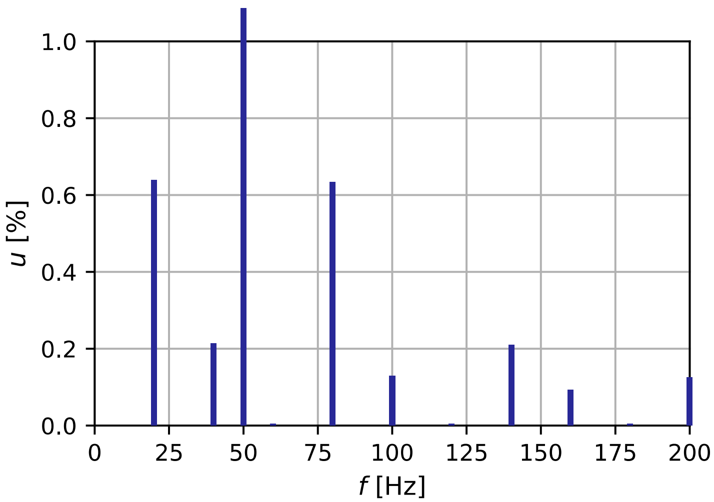

Fig. 4. Example of the test voltage spectrum for *DutyCyle* = 0.5
and the voltage modulation frequency, f_m = 30 Hz

An example of the instantaneous speed waveforms are shown in Figures 5 and 6 for voltage modulation frequency f_m = 30 Hz, and in Figures 7 and 8 for the frequency f_m = 45 Hz. The applied *DutyCycle* was equal to 0.5 (Fig. 5 and 7) and 0.25 (Fig. 6 and 8). For these parameters, *DutyCycle*, the speed waveforms significantly differ in shape.

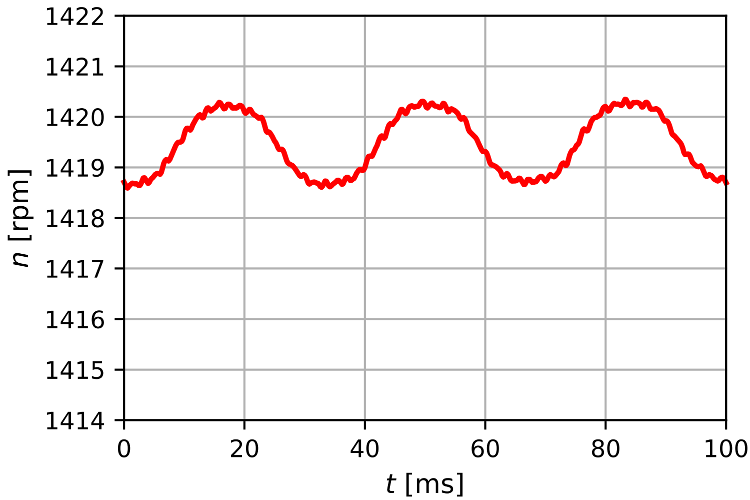

Fig. 5. Speed waveform for *DutyCycle* = 0.5
and the voltage modulation frequency, f_m = 30 Hz

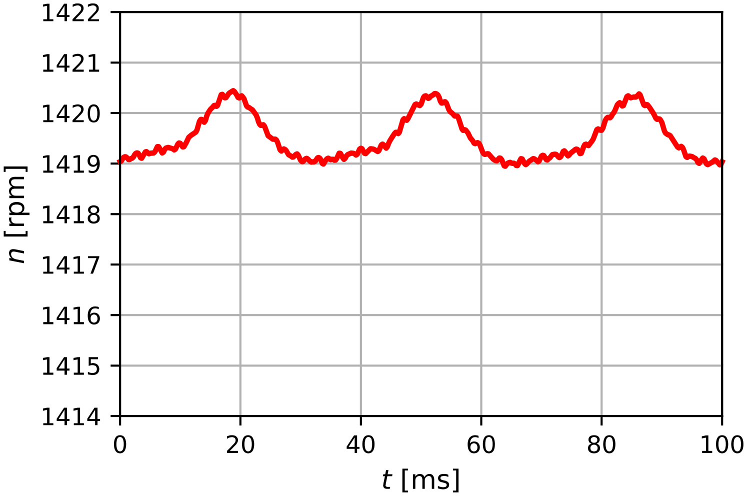

Fig. 6. Speed waveform for *DutyCycle* = 0.25
and the voltage modulation frequency, f_m = 30 Hz

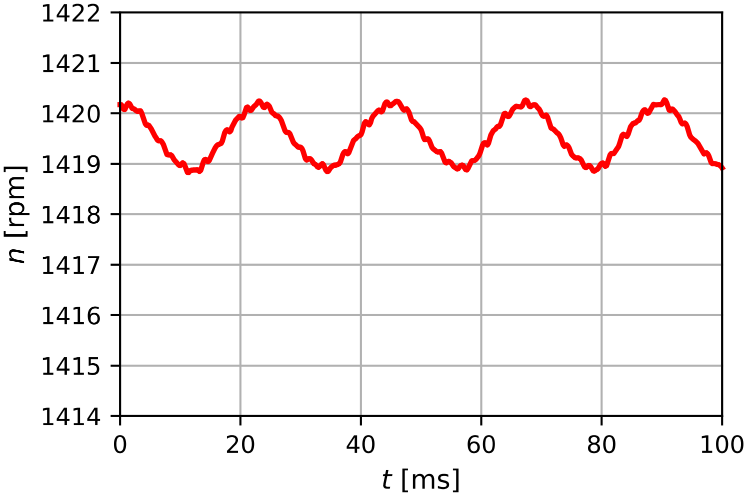

Fig. 7. Speed waveform for *DutyCycle* = 0.5
and the voltage modulation frequency, f_m = 45 Hz

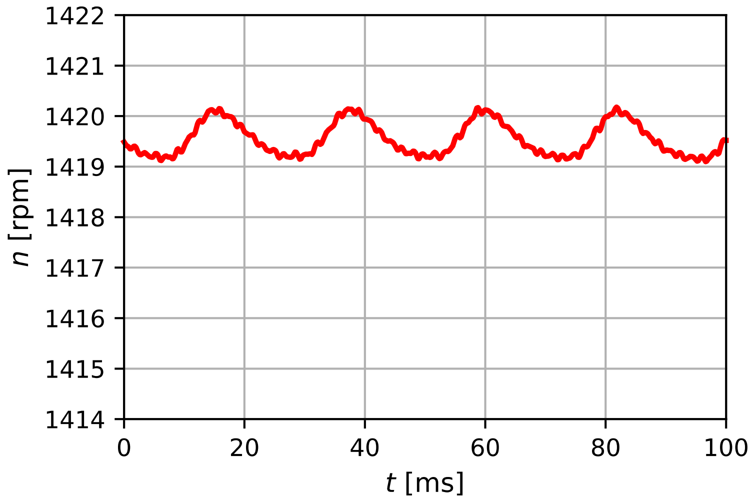

Fig. 8. Speed waveform for *DutyCycle* = 0.25
and the voltage modulation frequency, f_m = 45 Hz

The next diagram (Fig. 9) shows the amplitude of speed fluctuations versus voltage modulation frequency f_m and *DutyCycle*. The highest speed fluctuations occur for the modulation frequency f_m = 3 Hz and *DutyCycle* = 0.5, while the lowest for the modulation frequency with *DutyCycle* = 0 and *DutyCycle* = 1 (Fig. 9). Additionally, the local maxima of speed fluctuations appears for the modulation frequency f_m about 25–30 Hz.

Of note, the characteristics provided in Figure 9 show significant non-linarites, especially for a *DutyCycle* not equal to 0.25. They could be explained related to the various subharmonic and interharmonic content in the testing voltage for each modulation case.

For example, for *DutyCycle* = 0.25 and modulation frequency f_m < 25 Hz, the subharmonic caused by the second harmonic of the modulating function has a positive-sequence, while for the frequency f_m > 25 Hz it has a negative-sequence (based on Zhang, Xu and Liu 2005) and for f_m = 25 Hz it has a constant component.

Contrastingly, for *DutyCycle* = 0.5, the modulating function does not contain a second harmonic, but only odd harmonics.

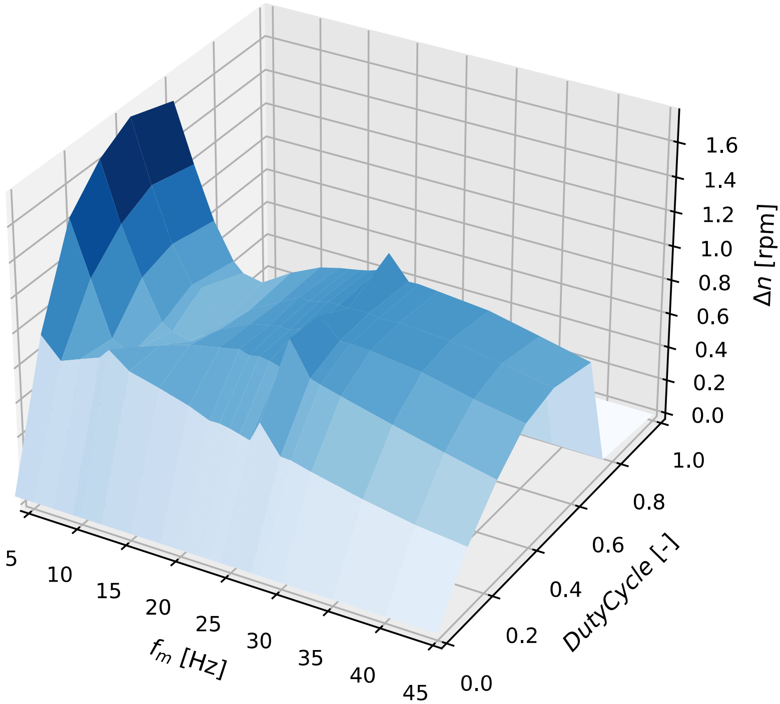

Fig. 9. Speed variation versus the frequency voltage modulation f_m and the *DutyCycle* parameter

The next figure (Fig. 10) presents the characteristics of the amplitude of the speed fluctuations versus the fill factor *DutyCycle*, for the frequencies f_m = 30 Hz and f_m = 45 Hz. For both frequencies f_m the highest speed fluctuations for *DutyCycle* are about 40–60%.

It should be added that *DutyCycle* = 0 or *DutyCycle* = 1 means no voltage fluctuations. Small speed fluctuations for these values of *DutyCycle* (Fig. 9) result from torque pulsations due to the presence of teeth and slots.

In summary, the fluctuations of the rotational speed non-linearly depend on the voltage modulation frequency. The fill factor *DutyCycle* considerably effects the shape of the speed waveforms.

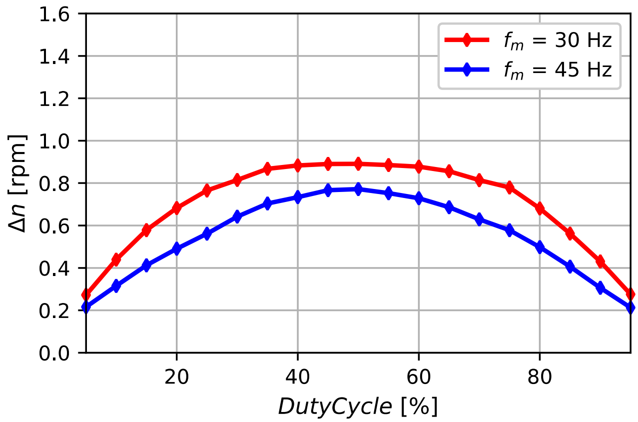

Fig. 10. Changes of the rotational speed versus *DutyCycle* for the voltage modulation frequencies, f_m = 30 Hz and f_m = 45 Hz

4. CONCLUSIONS

The test results demonstrate that speed fluctuations under a rectangular voltage modulation non-linearly depend on the modulation frequency. The fill factor value of the modulating signal considerably effects the shape of the speed waveforms. It could be explained using various contents of the voltage subharmonics and interharmonics for different cases of modulations. The results of the investigations should contribute to a better understanding of the phenomena occurring in the asynchronous motor under the condition of voltage fluctuation.

REFERENCES

Arkkio, A., Cederström, S., Awan, H.A.A., Saarakkala, S.E., Holopainen, T.P., 2018, *Additional Losses of Electrical Machines under Torsional Vibration*, IEEE Transactions on Energy Conversion, vol. 33, no. 1, pp. 245–251.

Bollen, M.H.J., Gu, I.Y.H., 2006, *Signal Processing of Power Quality Disturbances*, Wiley, New York, USA.

Crotti, G., D'Avanzo, G., Letizia, P.S., Luiso, M., 2021, *Measuring Harmonics with Inductive Voltage Transformers in Presence of Subharmonics*, IEEE Transactions on Instrumentation and Measurement, vol. 70, pp. 1–13.

EN Standard 50160, 2010, *Voltage Characteristics of Electricity Supplied by Public Distribution Network.*

Gallo, D., Landi, C., Langella, R., Testa, A., 2005, *Limits for Low Frequency Interharmonic Voltages: Can They Be Based on the Flickermeter Use?* IEEE Russia Power Tech, pp. 1–7.

Ghaseminezhad, M., Doroudi, A., Hosseinian, S.H., Jalilian, A., 2017a, *Analysis of Voltage Fluctuation Impact on Induction Motors by an Innovative Equivalent Circuit Considering the Speed Changes*, IET Generation Transmission and Distribution, vol. 11, pp. 512–519.

Ghaseminezhad, M., Doroudi, A., Hosseinian, S.H., Jalilian, A., 2017b, *An Investigation of Induction Motor Saturation under Voltage Fluctuation Conditions*, Journal of Magnetics, vol. 22, pp. 306–314.

Ghaseminezhad, M., Doroudi, A., Hosseinian, S.H., Jalilian, A., 2021a, *Analytical Field Study on Induction Motors under Fluctuated Voltages*, Iranian Journal of Electrical and Electronic Engineering, vol. 17, no. 1.

Ghaseminezhad, M., Doroudi, A., Hosseinian, S.H., Jalilian, A., 2021b, *High Torque and Excessive Vibration on the Induction Motors under Special Voltage Fluctuation Conditions*, COMPEL – The International Journal for Computation and Mathematics in Electrical and Electronic Engineering, vol. 40, no. 4, pp. 822–836.

Gnaciński, P., Hallmann, D., Klimczak, P., Muc, A., Pepliński, M., 2021, *Effects of Voltage Interharmonics on Cage Induction Motors*, Energies, vol. 14, no. 5.

Gnaciński, P., Hallmann, D., Pepliński, M., Jankowski, P., 2019a, *The Effects of Voltage Subharmonics on Cage Induction Machines*, International Journal of Electrical Power & Energy Systems, vol. 111, pp. 125–131.

Gnaciński, P., Klimczak, P., 2020, *High-Power Induction Motors Supplied with Voltage Containing Subharmonics*, Energies, vol. 13.

Gnaciński, P., Muc, A., Pepliński, M., 2021, *Influence of Voltage Subharmonics on Line Start Permanent Magnet Synchronous Motor*, IEEE Access, vol. 9, pp. 164 275–164 281.

Gnaciński, P., Pepliński, M., Hallmann, D., Jankowski, P., 2019b, *Induction Cage Machine Thermal Transients under Lowered Voltage Quality*, IET Electric Power Applications, vol. 13, no. 4, pp. 479–486.

Gnaciński, P., Pepliński, M., Murawski, L., Szeleziński, A., 2019c, *Vibration of an Induction Machine Supplied with Voltage Containing Subharmonics and Interharmonics*, IEEE Transactions on Energy Conversion, vol. 34, pp. 1928–1937.

Hallmann, D., 2020, *Analiza pracy sulnika indukcyjnego małej mocy zasilanego napięciem zawierającym subharmoniczne i interharmoniczne z wykorzystaniem modelu polowego*, rozprawa doktorska, Uniwersytet Morski w Gdyni, Gdynia 2020.

IEEE Standard 519-2014 (Revision of IEEE Standard 519-1992), 2014, IEEE *Recommended Practice and Requirements for Harmonic Control in Electric Power Systems*, New York, USA.

IEEE Standard 1453-2015, 2015, IEEE *Recommended Practice for the Analysis of Fluctuating Installations on Power Systems*, New York, USA.

Kovaltchouk, T., Armstrong, S., Blavette, A., Ahmed, H.B., Multon, B., 2016, *Wave Farm Flicker Severity: Comparative Analysis and Solutions*, Renewable Energy, vol. 91, pp. 32–39.

Kuwałek, P., 2021a, *Estimation of Parameters Associated with Individual Sources of Voltage Fluctuations*, IEEE Transactions on Power Delivery, vol. 36, no. 1, pp. 351–361.

Kuwałek, P., 2021b, *Selective Identification and Localization of Voltage Fluctuation Sources in Power Grids*, Energies, vol. 14, no. 20.

Kuwałek, P., 2022, IEC *Flickermeter Measurement Results for Distorted Modulating Signal while Supplied with Distorted Voltage*, 20th International Conference on Harmonics & Quality of Power (ICHQP), pp. 1-6.

Patel, D., Chowdhury, A., 2021, *Mitigation of Voltage Fluctuation in Distribution System using Sen Transformer with Variable Loading Conditions*, International Conference on Advances in Electrical, Computing, Communication and Sustainable Technologies (ICAECT), pp. 1–6.

Tennakoon, S., Perera, S., Robinson, D., 2008, *Flicker Attenuation, Part I: Response of Three-Phase Induction Motors to Regular Voltage Fluctuations*, IEEE Transactions on Power Delivery, vol. 23, pp. 1207–1214.

Testa, A., Akram, M.F., Burch, R., Carpinelli, G., Chang, G., et al., 2007, *Interharmonics: Theory and Modeling,* IEEE Transactions on Power Delivery, vol. 22, pp. 2335–2348.

Zhang, D., Xu, W., Liu, Y., 2005, *On the Phase Sequence Characteristics of Interharmonics*, IEEE Transactions on Power Delivery, vol. 20, no. 4, pp. 2563-2569.

Zhang, S., Kang, J., Yuan, J., 2021, *Analysis and Suppression of Oscillation in V/F Controlled Induction Motor Drive Systems*, IEEE Transactions on Transportation Electrification, vol. 8, pp. 1566–1574.